ORIGINAL RESEARCH

Aldosterone Promotes Cardiac Endothelial Cell Proliferation In Vivo

Basile Gravez, MSc; Antoine Tarjus, PhD; Véronique Pelloux, MSc; Antoine Ouvrard-Pascaud, PhD; Claude Delcayre, PhD; Janelise Samuel, MD, PhD; Karine Clément, MD, PhD; Nicolette Farman, MD, PhD; Fréderic Jaisser, MD, PhD;* Smail Messaoudi, PhD*

***Background*—**Experimentally, aldosterone in association with NaCl induces cardiac fibrosis, oxidative stress, and inflammation through mineralocorticoid receptor activation; however, the biological processes regulated by aldosterone alone in the heart remain to be identified.

***Methods and Results*—**Mice were treated for 7 days with aldosterone, and then cardiac transcriptome was analyzed. Aldosterone regulated 60 transcripts (51 upregulated and 9 downregulated) in the heart (fold change $\geq$1.5, false discovery rate $<$0.01). To identify the biological processes modulated by aldosterone, a gene ontology analysis was performed. The majority of aldosterone-regulated genes were involved in cell division. The cardiac Ki-67 index (an index of proliferation) of aldosterone-treated mice was higher than that of nontreated mice, confirming microarray predictions. Costaining of Ki-67 with vinculin, CD68, α-smooth muscle actin, CD31, or caveolin 1 revealed that the cycling cells were essentially endothelial cells. Aldosterone-induced mineralocorticoid receptor–dependent proliferation was confirmed ex vivo in human endothelial cells. Moreover, pharmacological-specific blockade of mineralocorticoid receptor by eplerenone inhibited endothelial cell proliferation in a preclinical model of heart failure (transverse aortic constriction).

***Conclusions*—**Aldosterone modulates cardiac gene expression and induces the proliferation of cardiac endothelial cells in vivo.
(*J Am Heart Assoc*. 2015;4:e001266 doi: 10.1161/JAHA.114.001266)

Key Words: aldosterone • heart • pressure overload • proliferation

Over the last 2 decades, there has been renewed interest in understanding the role of aldosterone and its receptor (the mineralocorticoid receptor [MR]) in cardiovascular function and disease due to the beneficial effects of pharmacological MR antagonists in patients with heart failure.[1–3]

In animal models, pharmacological blockade of MR reverses or prevents the adverse effects of aldosterone on cardiac fibrosis.[4,5] Experimentally, chronic infusion of aldosterone induces cardiac inflammation and fibrosis independently of increase in blood pressure.[4,5] Aldosterone also induces cardiac oxidative stress, mainly through activation of NADPH oxidases.[6] Noticeably, coadministration of NaCl is essential in these models: Aldosterone alone is not sufficient to induce cardiac fibrosis.

Beside fibrosis, aldosterone also alters cardiomyocyte calcium channel current,[7] impairs the activity of the ryanodine receptor,[8] and promotes arrhythmia.[9] In contrast to fibrosis and inflammation, the proarrythmogenic properties of aldosterone do not require coadministration of salt or a pathological environment. This suggests that aldosterone alone may establish conditions that sensitize cardiac tissue to other triggers; however, the biological processes activated by aldosterone in the heart in the absence of added sodium are far from being fully understood.

The aim of this study was to identify new aldosterone-regulated biological processes that might contribute to cardiac diseases. We used an approach consisting of pangenomic analysis of genes regulated in vivo in the mouse heart after administration of a low dose of aldosterone. Treatment duration was short (1 week) to favor the identification of primary aldosterone targets rather than those involved in compensatory or adaptive processes occurring after chronic administration of aldosterone. We report that moderate increase in plasma aldosterone concentration regulates cardiac expression of genes involved in proliferation and promotes proliferation of cardiac endothelial cells (ECs).

From the Inserm U1138, Team 1, 15 rue de l'école de médecine, Paris, France (B.G., A.T., N.F., F.J., S.M.); INSERM-UMR 1166 Team 6- GH Pitié-Salpêtrière, 83 Bd de l'hôpital, Paris, France (V.P., K.C.); UMR 644 Inserm-Université de Rouen. 22, Boulevard Gambetta, Rouen, France (A.O.-P.); Inserm U942, 41 Boulevard de la chapelle, Paris, France (C.D., J.S.).

*Dr Jaisser and Dr Messaoudi shared senior authorship.

Correspondence to: Smail Messaoudi, PhD, Centre de Recherche des Cordeliers, Equipe 1, Escalier E, 1er étage. 15 rue de l'Ecole de Médecine, 75006 Paris, France. E-mail: smail.messaoudi@crc.jussieu.fr

Received July 11, 2014; accepted November 20, 2014.

Moreover, pharmacological MR antagonism prevents endothelial proliferation observed in a rat model of heart failure.

Materials and Methods

Mice

Four-month-old male mice (B6D2) purchased from Janvier-Labs (Le Genest-Saint-Isle, France) were used for this study. The use of animals was in accordance with the guidelines of the European Community and approved by our institutional animal care and use committee and thus has been performed in accordance with the ethical standards laid down in the 1964 Declaration of Helsinki and its later amendments. Aldosterone (A9477; Sigma-Aldrich) was resuspended in ethanol, diluted 10× in saline, then infused (60 μg/kg per day) via osmotic minipumps (Alzet) (before minipump implantation, mice were anesthetized by xylasine or ketamine administration) for 1 week (n=6 to 9 per group) or 4 weeks (n=8 per group), as described previously.[10] This allowed a moderate increase in plasma aldosterone levels (5-fold increase, 2.9 nmol/L versus 0.6 nmol/L in control mice).[10] Infusion of the vehicle (ethanol 10% in saline) had no effects on the parameters studied.

Blood Pressure Measurement

Systolic blood pressure was measured by tail-cuff plethysmography in trained conscious mice using a BP-2000 Visitech system (Bioseb).

Tissue Sampling

Hearts were rinsed in cold PBS, weighed, and cut into 2 parts (transversal cut). The apex was frozen for mRNA and protein extraction. The base was immersed in Tissue-Tek (Sakura Finetek France) and frozen in liquid nitrogen-cooled isopentane for morphological studies. Kidneys were rinsed in cold PBS and weighed. All samples were frozen in liquid nitrogen and kept at −80°C.

Microarray and Gene Expression Analysis

Five mice per group were used to carry out microarray experiments (1 week aldosterone treatment). Total RNA was prepared from ventricle samples with the RNeasy Mini Kit (Qiagen), according to the manufacturer's instructions, and its quality was assessed with the 2100 Bioanalyzer (Agilent Technologies). Microarray experiments were carried out using the mouse GE 4x44K v2 microarray kit (Agilent Technologies). Labeling of the RNAs, hybridization (1 animal per array), and scanning of the microarrays were performed according to the manufacturer's instructions. Data were analyzed using GeneSpring software (Agilent Technologies). The false discovery rate and fold-change threshold retained were 1% and ≥1.5, respectively. Quantitative real-time polymerase chain reaction was carried out, as described previously.[11] Primer sequences are listed in Table 1.

Table 1. Primer Sequences

Genes	Forward Primer	Reverse Primer
18S	CGCCGCTAGAGGTGAAATTC	TCTTGGCAAATGCTTTCGC
Ang1	GAAGGGAACCGAGCCTACTC	ACCACCAACCTCCTGTTAGC
Birc5	GTGACGCCATCATGGGAGCTCC	AGGCTCGTTCTCGGTAGGGCAG
Ccnb1	TGATTTTGGAGGAGCCATGGCGCTC	GCACTCTTGCCTGTAGCTCTTCGC
Cdk1	AGTAACGAGCCGAGCCCAGCA	TCGGCCTTGCCAGAGCGTTTG
Fgf2	GCCAACCGGTACCTTGCTAT	GTCCCGTTTTGGATCCGAGT
Icam1	TCCGCTACCATCACCGTGTATTC	TGGCCTCGGAGACATTAGAGAAC
Mcp1	ATCCCAATGAGTAGGCTGGAGAGC	CAGAAGTGCTTGAGGTGGTTGTG
Neil3	ACCGCCGTTGTGTTCTCCGA	TGGAGCGCTTGCCATGTCTGC
Pgf	TCTGCTGGGAACAACTCA ACA	GTGAGACACCTCATCAGGGTAT
Tnfa	GGGACAGTGACCTGGACTGT	AGTGAATTCGGAAAGCCCATT
Ubc	AGCCCAGTGTTACCACCAAG	ACCCAAGAACAAGCACAAGG
Vcam	CTGGGAAGCTGGAACGAAGT	GCCAAACACTTGACCGTGAC
Vegf-a	AGCAACATCACCATGCAGATCATGC	TGAACAAGGCTCACAGTGAACGC

Ang1 indicates angiopoietin1; Birc5, Baculoviral IAP repeat containing 5; Ccnb1, cyclin B1; Cdk1, cyclin-dependent kinase 1; Fgf2, fibroblast growth factor 2; Icam1, intercellular adhesion molecule 1; Mcp1, macrophage chemo-attractant protein 1; Neil3, Nei like 3; Pgf, placental growth factor; Tnf-α, tumor necrosis factor α; UBC, ubiquitin; Vcam, vascular cell adhesion molecule 1; VEGF-a, vascular endothelial growth factor A.

Gene Ontology Analysis

Gene ontology (GO) analysis was carried using FunNet[12] (http://www.funnet.info/). FunNet integrates experimental gene expression data and knowledge about the biological roles of transcripts available in genomic annotation systems. Briefly, FunNet performs functional profiling of gene expression data to identify a set of significant (ie, overrepresented) biological themes characterizing the analyzed transcripts (ie, cellular processes, pathways, and molecular functions in which the analyzed transcripts are involved). The options provided with this type of analysis are related to the gene annotation systems to be used for functional profiling of transcripts and to the type of gene-enrichment computation performed for GO categories (ie, the 3 main conceptual axes of the GO lattice). The annotation systems currently available in FunNet are those provided by the Gene Ontology Consortium and the Kyoto Encyclopedia of Genes and Genomes.

Gene Network Building

The gene network was generated through the use of Ingenuity Pathway Analysis (Ingenuity Systems). A data set containing gene identifiers and corresponding expression values was uploaded into in the application. Each identifier was mapped to its corresponding object in the Ingenuity Knowledge Base. The genes, the expression of which was significantly differentially regulated, are called *network-eligible molecules* and were overlaid onto a global molecular network developed from information contained in the Ingenuity Knowledge Base. Networks of network-eligible molecules were then algorithmically generated based on their connectivity.

Immunofluorescence

Left ventricular frozen 4-μm sections were stained using primary antibodies against Ki-67 (ab15580; Abcam), CD31 (550274; BD Pharmigen), phospho-histone H3 (p-H3; CS9701; Cell Signaling), vinculin (V9131; Sigma-Aldrich), FITC-coupled caveolin 1 (sc894-FITC; Santa Cruz Biotechnology), α-smooth muscle actin isoform (ab7817; Abcam), and CD68 (ab53444; Abcam). Briefly, frozen sections were fixed in 4% paraformaldehyde and then washed with PBS Tween 20. Subsequently, sections were blocked with 5% bovine serum albumin for 30 minutes and incubated with the primary antibody overnight at 4°C. After rinsing with PBS, the sections were incubated for 1 hour with the appropriate secondary antibody. ECs and cycling or mitotic nuclei were identified with CD31 (or caveolin 1) and Ki-67 or p-H3 antibodies, respectively. Because Ki-67 and p-H3 are nuclear antigens and CD31 and caveolin1 are membrane proteins, Ki-67–positive and p-H3–positive nuclei are surrounded with CD31 or caveolin 1 staining. Vinculin antibody allowed the identification of cardiomyocyte outlines, whereas α-smooth muscle actin and CD68 antibodies detected smooth muscle cells and macrophages, respectively. A minimum of 5 fields per section was recorded at ×10 and ×20 using a Leica camera equipped with a fluorescent Leica DMR (Leica Microsystems). The Ki-67 or p-H3 index is defined as the number of positive Ki-67 or p-H3 nuclei per total nuclei. The numbers of capillaries and positive and total nuclei were determined using ImageJ (version 1.43) software. The capillary density was defined as the number of capillaries per surface unit.

Culture of Human Umbilical Vein Endothelial Cells and Aldosterone Treatment

Human umbilical vein ECs were purchased from ScienCell Research Laboratories (code 8000). Cells were grown in collagen-coated flasks with endothelial basal medium 2 supplemented with endothelial cell growth medium 2 (CC3162; Lonza). For experiments, cells were transferred into 6-well plates at a confluence of 15%. They were grown in serum-free medium 24 hours before stimulation. Aldosterone (Sigma-Aldrich) was initially dissolved in ethanol at a concentration of 10^{-3} mol/L. Cells were treated with aldosterone (10^{-8} mol/L) or vehicle (containing the same proportion of ethanol as treated cells) for 96 hours. Medium was renewed every 48 hours. To investigate the specificity of action of aldosterone, the MR antagonist spironolactone (S3378; Sigma-Aldrich) was used (dissolved in ethanol) at the final concentration of 10^{-6} mol/L.

Cell-Proliferation Assessment

Cell proliferation was assessed with the quick cell proliferation kit (65475; Biorad). Briefly, this assay is based on the cleavage of the tetrazolium salt WST-1 to formazan by cellular mitochondrial dehydrogenases. Expansion of viable cell numbers results in an increase in the overall activity of the mitochondrial dehydrogenases in the sample, corresponding to an increase in formazan dye metabolism. The formazan dye produced by the viable cells is measured at an absorbance of 440 nm using a standard multiwell spectrophotometer. Absorbance is directly proportional to the number of cells.

Thoracic Aortic Constriction and Eplerenone Treatment

Pressure overload was produced by thoracic aortic constriction, as previously described.[10] Briefly, 3-week-old male rats

(body weight 60±1 g) were anaesthetized with intraperitoneal injection of xylazine (50 mg/kg) and ketamine (100 mg/kg). Left ventricle pressure overload was then produced by coarctation of the ascending thoracic aorta with a partially occluded Weck Hemoclip. The same procedure was performed on sham-operated animals, but no clip was placed around the aorta. Animals were divided into 4 groups: (1) sham operated (n=5), (2) sham operated plus eplerenone (n=4), (3) pressure-overloaded rats (n=5), and (4) pressure-overloaded rats plus eplerenone (n=6). Animals were kept under identical housing conditions and sacrificed after 3 months. Eplerenone (E6657; Sigma-Aldrich), a specific MR blocker, was incorporated in food and available ad libitum.

Statistics

The results are reported as mean±SEM. The Shapiro–Wilk and Levene tests were used to analyze normality and variance or homogeneity of residuals, respectively. Statistical analysis was performed by *t* test or Mann–Whitney test. For aldosterone with or without spironolactone treatment on human umbilical vein ECs, we used a 2-factor ANOVA with repeated-measure analysis followed by Tukey's post hoc test. For the thoracic aortic constriction experiment, the Kruskal–Wallis test was performed. The Holm post hoc test was used to adjust for multiple comparisons. Statistical analysis was performed with SigmaPlot (version 11.0) software. Values of $P<0.05$ were considered statistically significant.

Results

Cardiac Transcriptome

One-week low-dose aldosterone infusion without increase in sodium intake did not alter blood pressure, body weight, or heart weight (Table 2). Transcriptomic analysis was performed on cardiac mRNA isolated from aldosterone-treated and control mice. Sixty-five probes corresponding to 60 transcripts (51 upregulated and 9 downregulated) (Figure 1A and 1B; Table 3) were differentially hybridized between aldosterone-treated and control mice (fold change of ≥1.5-fold and false discovery rate <1%). The microarray data were confirmed by quantitative polymerase chain reaction (Figure 1C).

Gene Ontology Analysis

We then performed a GO analysis of the upregulated transcripts to identify the biological processes modulated by aldosterone (the number of transcripts downregulated was too low to perform a significant GO analysis). The GO analysis was based on National Center for Biotechnology Information Entrez Gene identifier (which allows unambiguous identification of transcripts) in a manner that transcripts identified more than once (with different probe names) did not artificially enrich a GO category. Among the 51 aldosterone-upregulated transcripts, 43 have at least 1 GO biological process annotation; therefore, the rate of coverage was 84%. Aldosterone-regulated cardiac transcripts were overrepresented in GO categories involved in cell proliferation (cell cycle, cell division, mitosis) (Figure 2A). For example, 66% of aldosterone-regulated transcripts were annotated with the *cell cycle* GO biological process annotation. Only 0.04% of the annotated transcripts on the microarray (494 of 14 021) were marked with this annotation, indicating very significant enrichment of this category ($P<0.0001$).

Cardiac Proliferation Assessment

We assessed cell proliferation in cardiac sections of aldosterone-treated (1 week) and control mice, probing Ki-67 as a marker of cell cycle activity[13] and p-H3 as a marker of mitotic activity[14] (Figure 2B). Absolute numbers of Ki-67 antigen-labeled cells were consistently higher than those of p-H3–labeled cells. Ki-67 protein is present during all active phases of the cell cycle (G_1, S, G_2, and mitosis), whereas histone H3 is phosphorylated only during mitosis.[13,14] Aldosterone increased Ki-67 index by 300% ($P<0.05$) (Figure 2C). Similar

Table 2. General Characteristics of Mice

	1 Week		4 Weeks	
	Control (n=6)	Aldo (n=9)	Control (n=8)	Aldo (n=8)
Body weight, g	27.9±0.4	28.7±0.4	33.9±0.6	32.9±0.2
Heart weight, mg	132.5±3.1	136.9±3.0	172.3±5.4	176.2±4.1
Blood pressure, mm Hg	126.1±3.1	127.2±2.4	127.3±2.4	131.6±1.8

Values are Mean±SEM. Aldo indicates aldosterone.

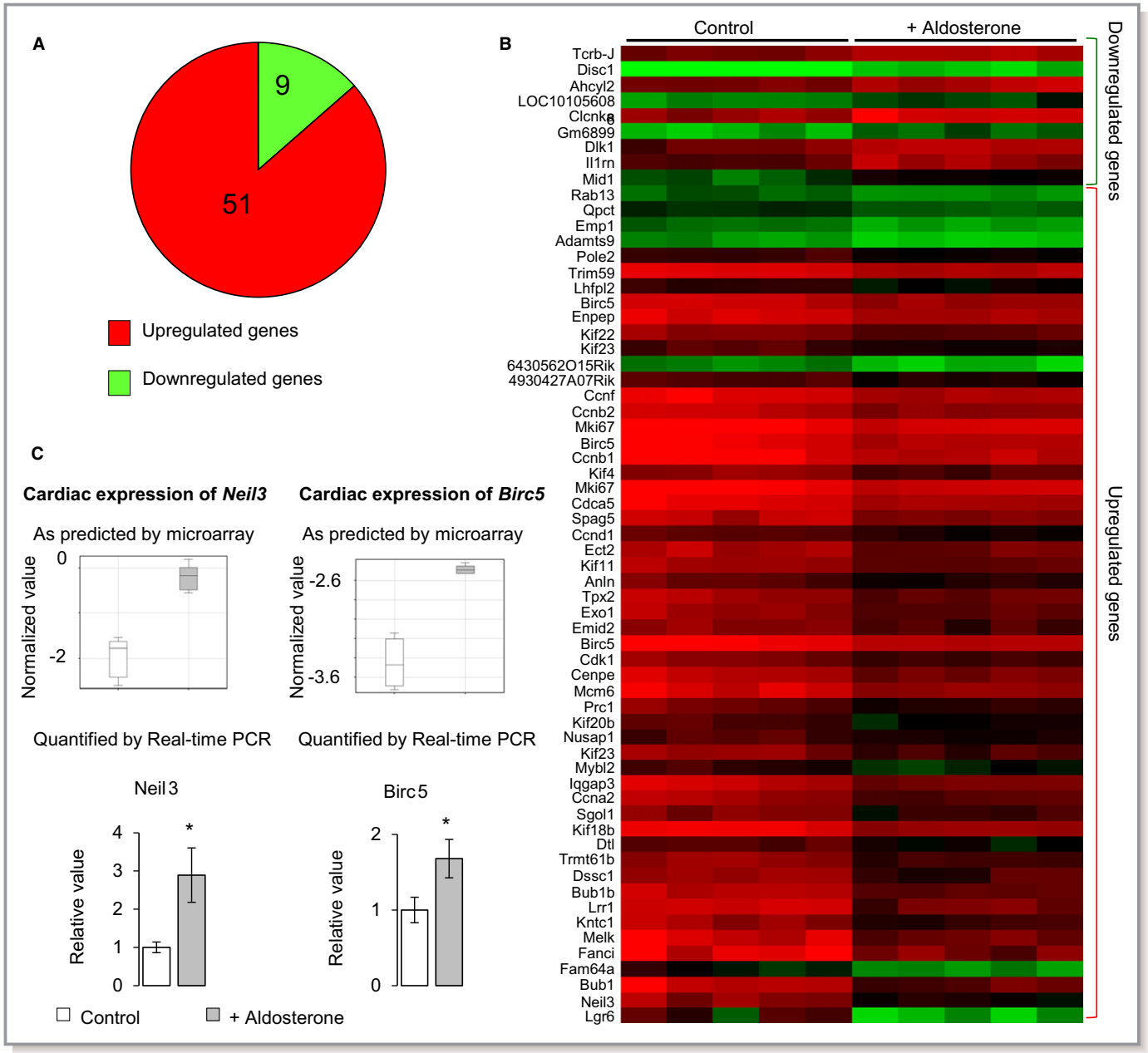

Figure 1. A, Schematic representation of aldosterone-regulated genes, as predicted by microarray analysis. Aldosterone (1-week treatment) regulated 60 genes: 51 were upregulated, and 9 were downregulated (fold change ≥1.5, false discovery rate <1%). B, Heat map of microarray-predicted aldosterone-regulated genes. Genes are classified according to the fold change of the genes. C, Genes tested to validate aldosterone-regulated genes as predicted by microarrays (top of the panel; control n=5 and aldosterone n=5). The expression of these genes was assessed by quantitative real-time PCR and confirmed microarray results (bottom of the panel, Ctrl n=6 and Aldo n=9). Statistical analysis was performed using the Mann–Whitney test. Mean±SEM. *P<0.05. PCR indicates polymerase chain reaction.

variation was observed with p-H3 cardiac immunostaining (Figure 2C).

Master Genes

To identify genes possibly involved in aldosterone-induced cardiac cell proliferation, we proceeded to a network analysis. The network was generated from the aldosterone-regulated genes through the use of an Ingenuity Pathway Analysis system. Among the 60 aldosterone-regulated genes, 28 were eligible to build a network based on the Ingenuity Knowledge Base. Among the genes used to build the network, we focused on those interacting with the greatest number of other genes in the cytoplasm—cyclin B1 (*Ccnb1*), with 10 interactions—and the nuclei—cyclin dependent kinase 1 (*Cdk1*), with 16 interactions (Figure 2D). These genes play crucial roles in cell

Table 3. Aldosterone-Regulated Genes in the Heart

Gene Symbol	Reg	*P* Value	FC	Description
Tcrb-J	Down	0.0043	1.73	*Mus musculus* rearranged T-cell receptor beta variable region (Vb17a). [X61758]
Disc1	Down	0.0048	1.74	Disrupted in schizophrenia 1 [ENSMUST00000122389]
Ahcyl2	Down	0.0065	1.81	S-adenosylhomocysteine hydrolase-like 2 [ENSMUST00000150365]
LOC101056086	Down	0.0069	1.86	PREDICTED: uncharacterized LOC101056086 (LOC101056086), [XM_003945428]
Clcnka	Down	0.0079	1.90	Chloride channel Ka (Clcnka), TV 1, [NM_024412]
Gm6899	Down	0.007	2.00	Adult male corpora quadrigemina cDNA, RIKEN full-length enriched library, clone:B230320C11 product:hypothetical protein, full insert sequence. [AK140159]
Dlk1	Down	0.0069	2.03	Delta-like 1 homolog (Drosophila), TV 1, [NM_010052]
Il1rn	Down	0.0089	2.08	Interleukin 1 receptor antagonist, TV 2, [NM_001039701]
Mid1	Down	0.0047	2.21	Midline 1 [ENSMUST00000149258]
Rab13	Up	0.0069	1.51	Adult male corpora quadrigemina cDNA, RIKEN full-length enriched library, clone:B230212B15 product:GTP-binding protein rab13 (fragment) homolog [Rattus norvegicus], full insert sequence. [AK080805]
Qpct	Up	0.0024	1.51	Glutaminyl-peptide cyclotransferase (glutaminyl cyclase), [NM_027455]
Emp1	Up	0.0061	1.55	Epithelial membrane protein 1, [NM_010128]
Adamts9	Up	0.0073	1.55	A disintegrin-like and metallopeptidase (reprolysin type) with thrombospondin type 1 motif, 9, [NM_175314]
Pole2	Up	0.0049	1.56	Polymerase (DNA directed), epsilon 2 (p59 subunit), [NM_011133]
Trim59	Up	0.0035	1.57	Tripartite motif-containing 59, [NM_025863]
Lhfpl2	Up	0.0069	1.62	Lipoma HMGIC fusion partner-like 2, [NM_172589]
Birc5	Up	0.0061	1.62	Baculoviral IAP repeat-containing 5, TV 1, [NM_009689]
Enpep	Up	0.0047	1.63	Glutamyl aminopeptidase, [NM_007934]
Kif22	Up	0.0069	1.65	Kinesin family member 22, [NM_145588]
Kif23	Up	0.0089	1.68	Kinesin family member 23, [NM_024245]
6430562O15Rik	Up	0.0081	1.69	Adult male olfactory brain cDNA, RIKEN full-length enriched library, clone:6430562O15 product:unclassifiable, full insert sequence. [AK032482]
4930427A07Rik	Up	0.0047	1.72	RIKEN cDNA 4930427A07 gene, [NM_134041]
Ccnf	Up	0.0049	1.75	Cyclin F, [NM_007634]
Ccnb2	Up	0.0062	1.77	Cyclin B2, [NM_007630]
Mki67	Up	0.0085	1.77	Antigen identified by monoclonal antibody Ki 67, [NM_001081117]
Birc5	Up	0.0057	1.77	Baculoviral IAP repeat-containing 5, TV 3, [NM_001012273]
Ccnb1	Up	0.0067	1.82	Cyclin B1, [NM_172301]
Kif4	Up	0.0057	1.83	Kinesin family member 4, [NM_008446]
Mki67	Up	0.0083	1.84	Antigen identified by monoclonal antibody Ki 67, [NM_001081117]
Cdca5	Up	0.0024	1.85	Cell division cycle associated 5, [NM_026410]
Spag5	Up	0.0062	1.88	Sperm associated antigen 5, [NM_017407]
Ccnd1	Up	0.0035	1.90	Cyclin D1, [NM_007631]
Ect2	Up	0.0074	1.90	Ect2 oncogene, TV 1, [NM_007900]
Kif11	Up	0.0024	1.92	Kinesin family member 11, [NM_010615]
Anln	Up	0.0073	1.93	Anillin, actin binding protein, [NM_028390]
Tpx2	Up	0.0079	1.93	TPX2, microtubule-associated protein homolog (*Xenopus laevis*), TV 2, [NM_028109]
Exo1	Up	0.0062	1.93	Exonuclease 1, [NM_012012]
Emid2	Up	0.0065	1.94	EMI domain containing 2 [ENSMUST00000111103]
Birc5	Up	0.0024	1.95	Baculoviral IAP repeat-containing 5, TV 3, [NM_001012273]

Continued

Table 3. Continued

Gene Symbol	Reg	*P* Value	FC	Description
Cdk1	Up	0.0047	1.98	Cyclin-dependent kinase 1, [NM_007659]
Cenpe	Up	0.0064	2.00	Centromere protein E, [NM_173762]
Mcm6	Up	0.0047	2.01	Minichromosome maintenance deficient 6 (MIS5 homolog, *Saccharomyces pombe*) (*Saccharomyces cerevisiae*), [NM_008567]
Prc1	Up	0.0069	2.05	Protein regulator of cytokinesis 1, [NM_145150]
Kif20b	Up	0.0069	2.06	Kinesin family member 20B, [NM_183046]
Nusap1	Up	0.0057	2.08	Nucleolar and spindle associated protein 1, TV 1, [NM_133851]
Mybl2	Up	0.0073	2.13	Myeloblastosis oncogene-like 2, [NM_008652]
Iqgap3	Up	0.0065	2.13	IQ motif containing GTPase activating protein 3, [NM_001033484]
Ccna2	Up	0.0047	2.16	Cyclin A2, [NM_009828]
Sgol1	Up	0.0047	2.18	Shugoshin-like 1 (*Saccharomyces pombe*), [NM_028232]
Kif18b	Up	0.0089	2.27	Kinesin family member 18B, [NM_197959]
Dtl	Up	0.0003	2.28	Denticleless homolog (Drosophila), [NM_029766]
Trmt61b	Up	0.0035	2.28	tRNA methyltransferase 61B, TV 2, non-coding RNA [NR_027952]
Dscc1	Up	0.0016	2.29	Defective in sister chromatid cohesion 1 homolog (*Saccharomyces cerevisiae*), [NM_183089]
Olfr631	Up	0.0064	2.46	Olfactory receptor 631, [NM_001271020]
Bub1b	Up	0.0003	2.47	Budding uninhibited by benzimidazoles 1 homolog, beta (*Saccharomyces cerevisiae*), [NM_009773]
Lrr1	Up	0.0047	2.59	Leucine rich repeat protein 1, [NM_001081406]
Kntc1	Up	0.0047	2.76	Kinetochore associated 1, [NM_001042421]
Melk	Up	0.0049	2.92	Maternal embryonic leucine zipper kinase, [NM_010790]
Fanci	Up	0.0065	2.95	Fanconi anemia, complementation group I, [NM_145946]
Fam64a	Up	0.0049	2.95	Family with sequence similarity 64, member A, [NM_144526]
Bub1	Up	0.0061	2.96	Budding uninhibited by benzimidazoles 1 homolog (*Saccharomyces cerevisiae*), TV 2, [NM_009772]
Neil3	Up	0.0027	3.36	Nei like 3 (*Escherichia coli*), [NM_146208]
Lgr6	Up	0.0065	6.28	Adult male aorta and vein cDNA, RIKEN full-length enriched library, clone:A530037C04 product:CDNA FLJ14471 FIS, CLONE MAMMA1001030, WEAKLY SIMILAR TO LUTROPIN-CHORIOGONADOTROPIC HORMONE RECEPTOR homolog [*Homo sapiens*]. [AK040883]

Some genes appear more than 1 time because the different probe corresponding to these genes have been differentially hybridized between aldosterone-treated and control mice.
FC indicates absolute fold change; *P,* corrected *P* value; Reg, regulation; TV, transcript variant.
Accession number: for all the genes, accession number provided is the National Center for Biotechnology Information GenBank accession number, except for Disc1, Ahcyl2, Mid1, and Emid2, which is the Ensembl accession number.

cycling and proliferation. Consistent with Ki-67 increased index, quantitative polymerase chain reaction confirmed that cardiac expression of these genes was significantly increased by aldosterone (Figure 2E).

Identification of the Cycling Cells

To identify the cell type that proliferates on aldosterone infusion, we performed double immunostaining of cardiac sections from aldosterone-treated and control mice. In aldosterone-treated mice, Ki-67–positive nuclei were localized around the cardiomyocytes that were delineated by vinculin immunostaining (Figure 3). Very few Ki-67–positive nuclei colocalized with the α-smooth muscle actin (a smooth muscle cell marker) or CD68 (a macrophage marker) (Figure 3). The majority of Ki-67–positive nuclei were colocalized within CD31-positive cells, indicating that most of the activated cells were ECs (Figure 4A). Similar results were obtained with caveolin 1, another marker of ECs (Figure 4A). P-H3 was also colocalized within caveolin 1–positive cells, strengthening our previous observation (Figure 4A). Caveolin 1 specificity for ECs was assessed by double immunostaining of ECs with CD31 and caveolin 1 (Figure 4B). We conclude that aldosterone promotes EC proliferation in vivo.

Cardiac expression of several proangiogenic growth factors (vascular endothelial growth factor A [VEGFA], placental growth factor [PGF], angiopoietin 1 [ANG1], and fibroblast growth factor 2 [FGF2]) was not significantly altered by aldosterone treatment for 1 week (Figure 4C). Similarly, the expression of proinflammatory molecules (tumor necrosis

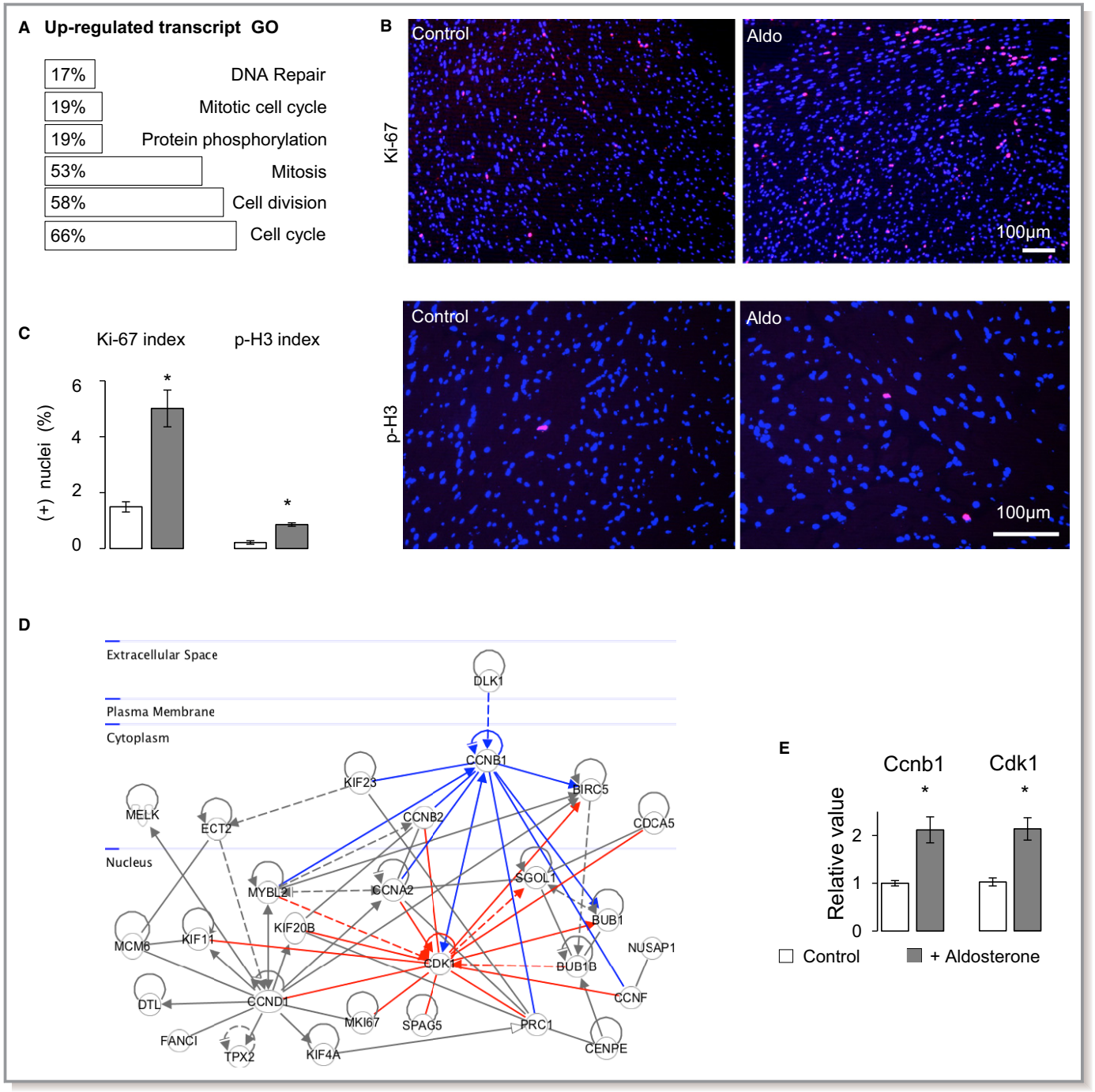

Figure 2. A, Gene ontology analysis of aldosterone-upregulated genes with FunNet software. Aldosterone-upregulated genes were overrepresented in gene ontology categories involved in cell cycle, proliferation, and mitosis. B, Ki-67 and p-H3 immunolabeling of cardiac sections (4 µm) of aldosterone-treated and control mice. In blue, DAPI-stained nuclei; in red, Ki-67 positive nuclei. C, Cardiac Ki-67 and p-H3 index quantification. Aldosterone induced an increase in cardiac Ki-67 and p-H3 indexes in mice (control n=6 and aldosterone n=9). D, The network was generated using Ingenuity Pathway Analysis software from the aldosterone-regulated genes. Cyclin B1 (*Ccnb1*) and cyclin dependent kinase 1 (*Cdk1*) (highlighted in red) were the most connected genes. E, Cardiac expression of *Ccnb1* and *Cdk1* genes was increased by aldosterone. Expression of these genes was assessed by quantitative real-time polymerase chain reaction (normalized to 18S and ubiquitin C genes) (control n=6 and aldosterone n=9). Statistical analysis was performed by Mann–Whitney test. Mean±SEM. **P*<0.05 vs controls. Aldo indicates aldosterone; DAPI, 4′,6-diamidino-2-phenylindole; p-H3, phospho-histone H3.

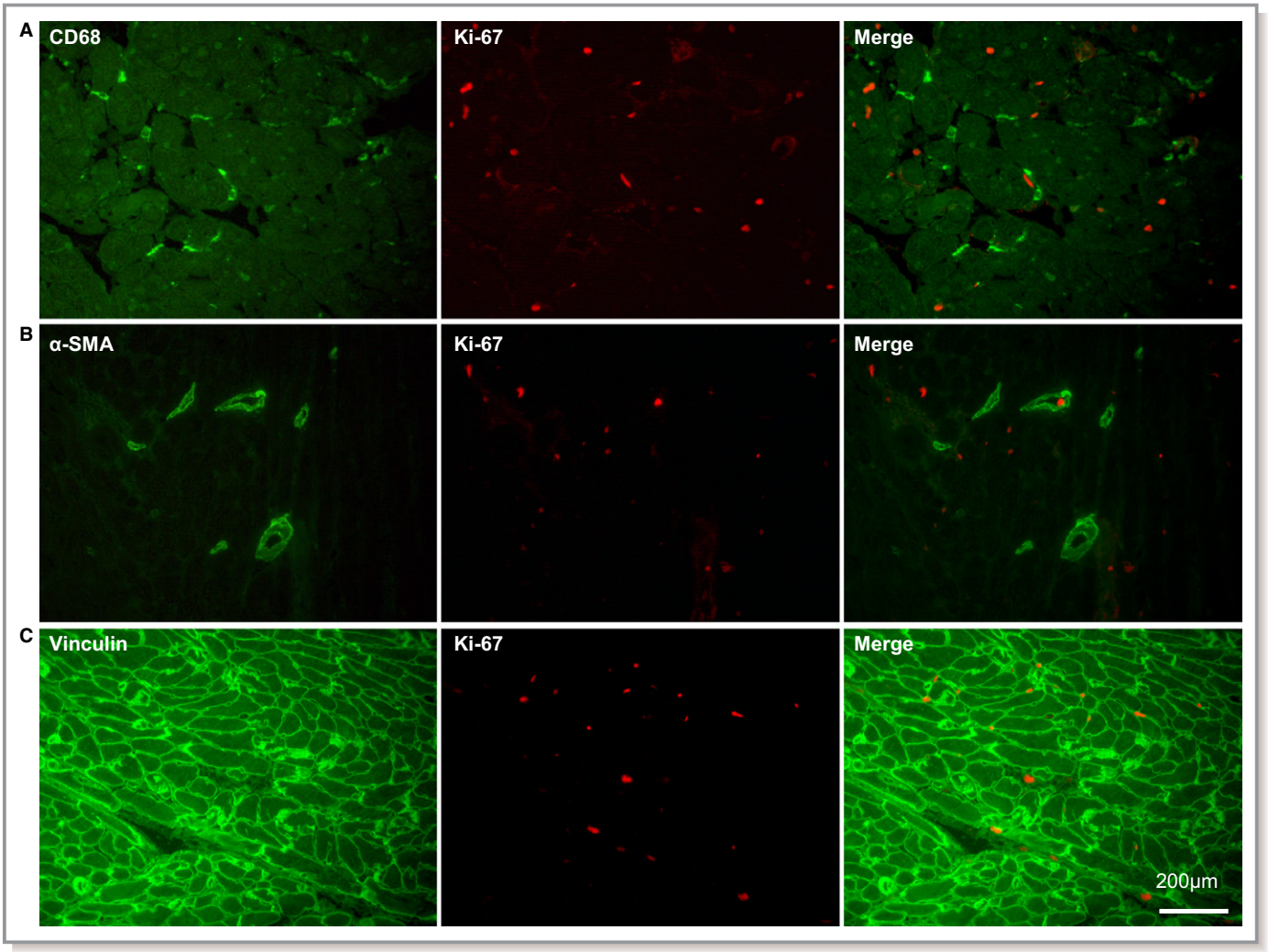

Figure 3. Double immunolabeling of cardiac sections from aldosterone-treated mice. Cardiac sections (4 μm) were labeled with anti-Ki-67 and anti-CD68 (A), α-SMA (B) or vinculin (C) antibodies. Ki-67–positive nuclei were localized all around cardiomyocytes in the interstitium. Very few Ki-67–positive nuclei colocalized with α-SMA or CD68. α-SMA indicates α-smooth muscle actin.

factor α, macrophage chemoattractant protein 1, intercellular adhesion molecule 1 [ICAM-1], and vascular cell adhesion molecule 1) that have been associated with proangiogenic properties of aldosterone in the retina[15] was not altered (Figure 4C).

Aldosterone induction of EC proliferation was further studied ex vivo in human umbilical vein ECs. Aldosterone (10^{-8} mol/L) enhanced human umbilical vein EC proliferation in a time-dependent manner. This effect was MR dependent because it was prevented by spironolactone addition (Figure 4D).

Aldosterone Induces Angiogenesis in the Heart

To study whether increase in EC proliferation was accompanied by angiogenesis, we analyzed capillary density. No modifications were detected after 1 week of aldosterone treatment. Longer treatment (4 weeks) did not alter blood pressure and body weight (Table 2). The heart was not hypertrophied, but capillary density was significantly increased, albeit to a limited extent (+7%, $P<0.05$) (Figure 5A and 5B). The expression of Ccnb1 and Cdk1 was not altered, whereas Ki-67 index was moderately increased (+38%, $P<0.05$; less than after 1 week treatment [+300%] [Figure 2C]) (Figure 5C and 5D). Expression of *VegfA* was increased (+40%, $P<0.005$), whereas expression of *Pgf*, *Ang1*, and *Fgf2* was not (Figure 5E).

Endothelial Cell Proliferation in Heart Failure

To study whether aldosterone may play a role in cardiac pathologies by promoting EC proliferation, we used a model of heart failure in rat (thoracic aortic constriction) that we characterized in a previous study.[10] Thoracic aortic constriction induced an increase in Ki-67 index (+61%, $P<0.05$) that

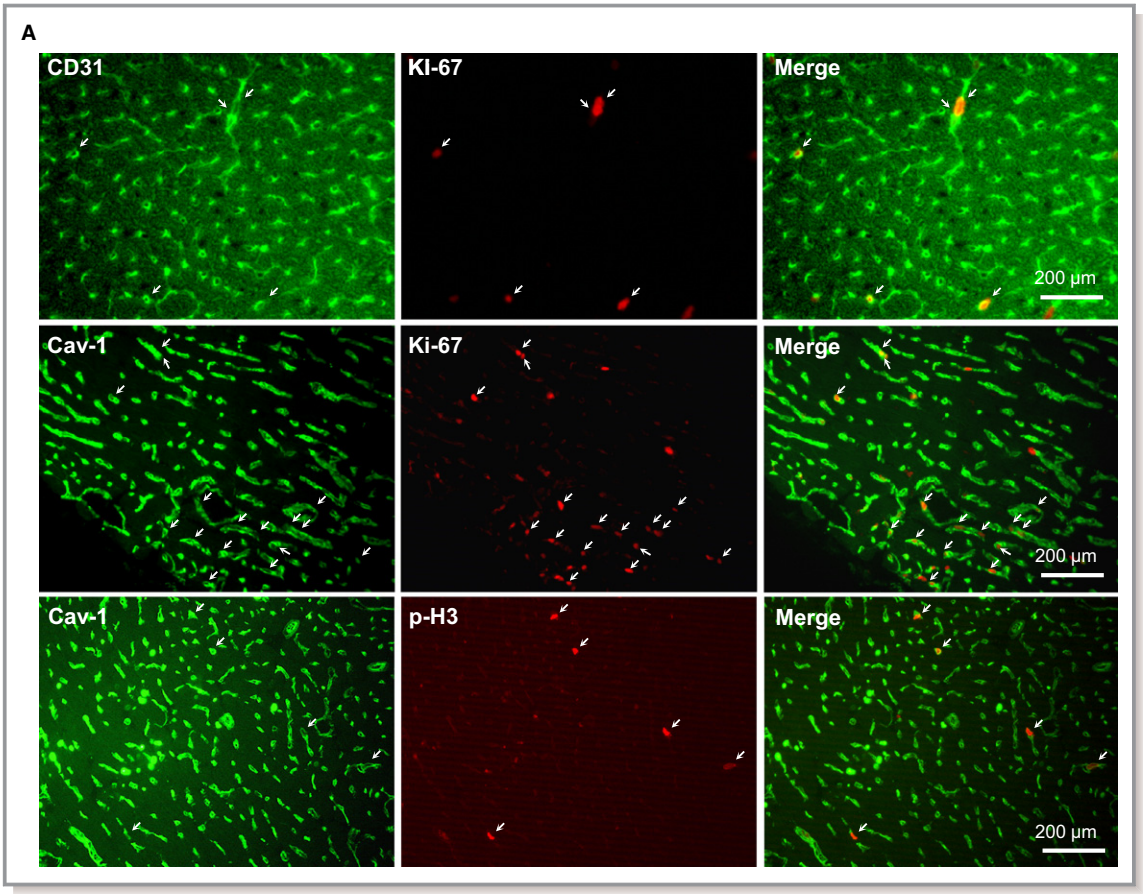

Figure 4. A, Double immunolabeling of cardiac sections from aldosterone-treated mice (1 week). Cardiac sections (4 µm) were labeled with anti-Ki-67 and either anti-CD31 or anti-Cav-1 antibodies. Sections were also colabeled with anti-p-H3 and Cav-1. A very large fraction of Ki-67 positive nuclei colocalized within CD31 and Cav-1–positive cells, indicating that most of the activated cells were endothelial cells. P-H3–positive nuclei also colocalized within Cav-1 positive cells. B, Double immunolabeling of cardiac sections. Cardiac sections (4 µm) were labeled with anti-CD31 and anti-Cav-1 antibodies. All CD31 (+) cells are positives for Cav-1 expression, and all Cav-1 (+) cells are positives for CD31 expression. Cav-1 is thus specific for endothelial cells. C, Cardiac expression of proangiogenic genes (angiopoietin1 [*Ang1*], fibroblast growth factor 2 [*Fgf2*], placental growth factor [*Pgf*], and vascular endothelial growth factor A [*Vegf-a*] and pro-inflammatory tumor necrosis factor α [*Tnf-α*], macrophage chemo-attractant protein 1 [*Mcp1*], vascular cell adhesion molecule 1 [*Vcam1*], and intercellular adhesion molecule 1 [*Icam1*]) was not increased by aldosterone. Expression of these genes was assessed by Q-PCR (normalized to 18S and ubiquitin C genes) (control n=6 and aldosterone n=9). Statistical analysis was performed by Mann–Whitney test. Mean±SEM. **P*<0.05 vs controls. D, Assessment of endothelial cells (HUVEC) proliferation. HUVEC were treated with 10^{-8} mol/L aldosterone (with or without spironolactone 10^{-6} mol/L) for 48 to 96 hours. Cell number was assessed by measurement of the absorbance of medium at 440 nm after the cleavage of the tetrazolium salt WST-1 to formazan by viable cells. Aldosterone induces an increase in cell number at 96 hours. This effect is abolished by spironolactone (6 wells per condition). Statistical analysis was performed by 2-factor ANOVA with repeated measures, followed by Tukey's post hoc test. Mean±SEM. **P*<0.05 vs untreated cells; †*P*<0.05 vs spironolactone-treated cells. Aldo indicates aldosterone; Cav-1 indicates caveolin 1; Ctrl, control; HUVEC, human umbilical vein endothelial cells; p-H3, phospho-histone H3; Q-PCR, quantitative real-time polymerase chain reaction; spi, spironolactone.

was normalized by eplerenone, a specific MR blocker (Figure 6A). Most of the Ki-67–positive cells colocalized within caveolin 1–positive cells, indicating that proliferating cells were endothelial (Figure 6B). Consequently, in this model of heart failure, MR activation participates in proliferation of ECs.

Discussion

Using a strategy coupling pharmacological and genomic approaches, this study demonstrates that a modest increase in plasma aldosterone concentration that is within the pathophysiological range induces expression of genes

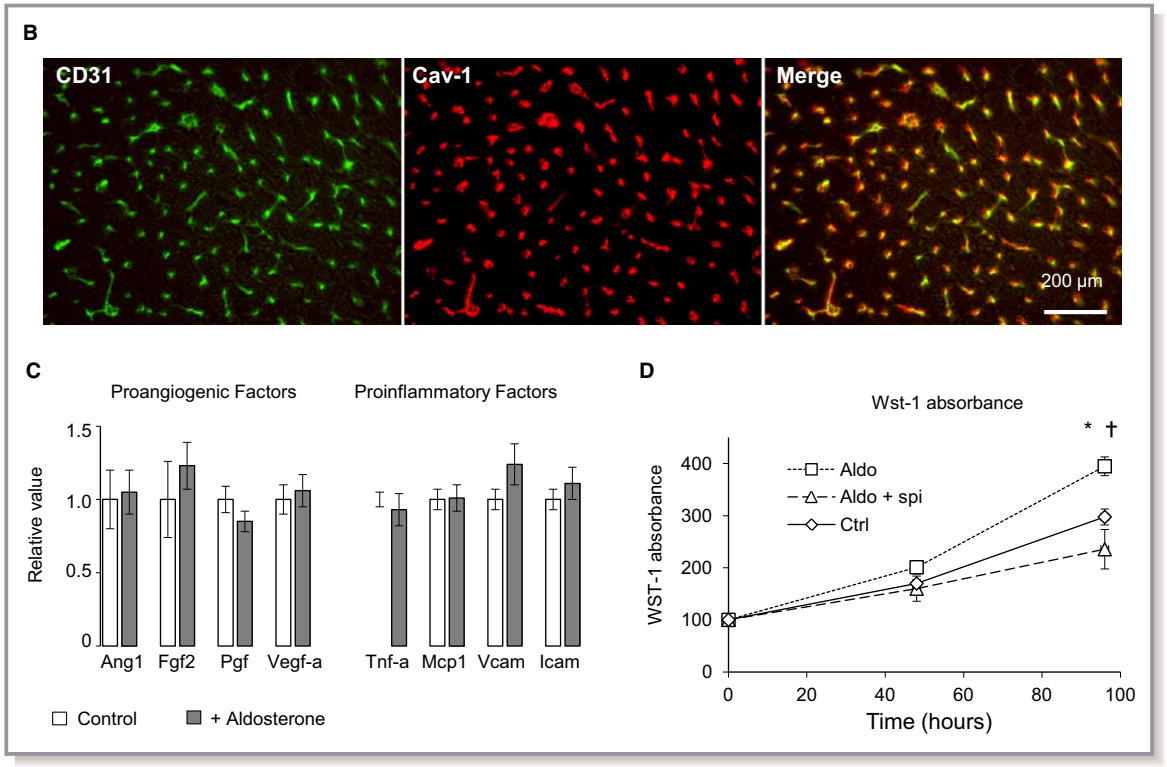

Figure 4. Continued

involved in cell cycle and promotes cardiac EC proliferation after 1 week and angiogenesis after 4 weeks.

The effects of aldosterone on ECs and angiogenesis are controversial. In mice, aldosterone impairs ECs sprouting from vascular segments.[16] In rats, aldosterone decreased the number of circulating endothelial progenitor cells,[17] and in patients with hyperaldosteronism, the number of circulating endothelial progenitor cells was inversely correlated with plasma aldosterone concentration.[18] Proliferative effects have also been reported in vivo: Aldosterone enhances neovascularization in an experimental model of ischemia,[19] prevents capillary rarefaction in a model of type 1 diabetes,[20] and stimulates pathological angiogenesis in the retina.[21] Ex vivo studies suggest that this apparent paradox may be dose dependent. At high concentrations (10^{-5} to 10^{-6} mol/L, far above pathological conditions), aldosterone attenuated human endothelial progenitor cell proliferation and angiogenesis, whereas lower concentrations (10^{-9} to 10^{-8} mol/L, the biological range) of aldosterone enhanced endothelial progenitor cell and retinal EC proliferation.[18,21] Furthermore, at pathophysiological concentrations (10^{-9} to 10^{-8} mol/L), aldosterone increased the formation of tubules by bovine retinal ECs in addition to promoting their proliferation.[21] In addition to the dose, in vivo treatment duration and confounding factors (eg, pathologies such as diabetes and heart failure) are parameters that might explain these apparent discrepancies in the literature. Further studies are required for a better understanding of the paradoxical angiogenic properties of aldosterone.

The pathophysiological consequences of aldosterone-dependent increase in cardiac EC proliferation are unknown. ECs are crucial for heart function by regulating vascular permeability, modulating the diameter of blood vessels in response to hemodynamic and hormonal stimuli, regulating leukocyte recruitment and adhesion, and preventing blood coagulation.[22] Several ex vivo studies demonstrated that aldosterone regulates EC functions. In coronary ECs, aldosterone induces the expression of proinflammatory molecules as ICAM-1 and promotes leukocyte adhesion.[23] In human umbilical vein ECs, aldosterone modulates endothelial permeability and endothelial nitric oxide synthase activity.[24] We report in this paper that ECs are also sensitive to a low concentration of aldosterone in vivo and that they are targets of aldosterone in the heart. By activating ECs and promoting their proliferation, aldosterone may alter the finely tuned complex balance of interactions of ECs with their immediate environment and thus may sensitize the cardiac tissue to other triggers such as salt, oxidative stress, or increased blood pressure. Furthermore, the pathophysiological consequences of aldosterone-induced EC proliferation may depend on the environment. In rat, we showed that EC proliferation is increased after thoracic aortic constriction, an effect inhibited by MR blockade. Teekakirikul and

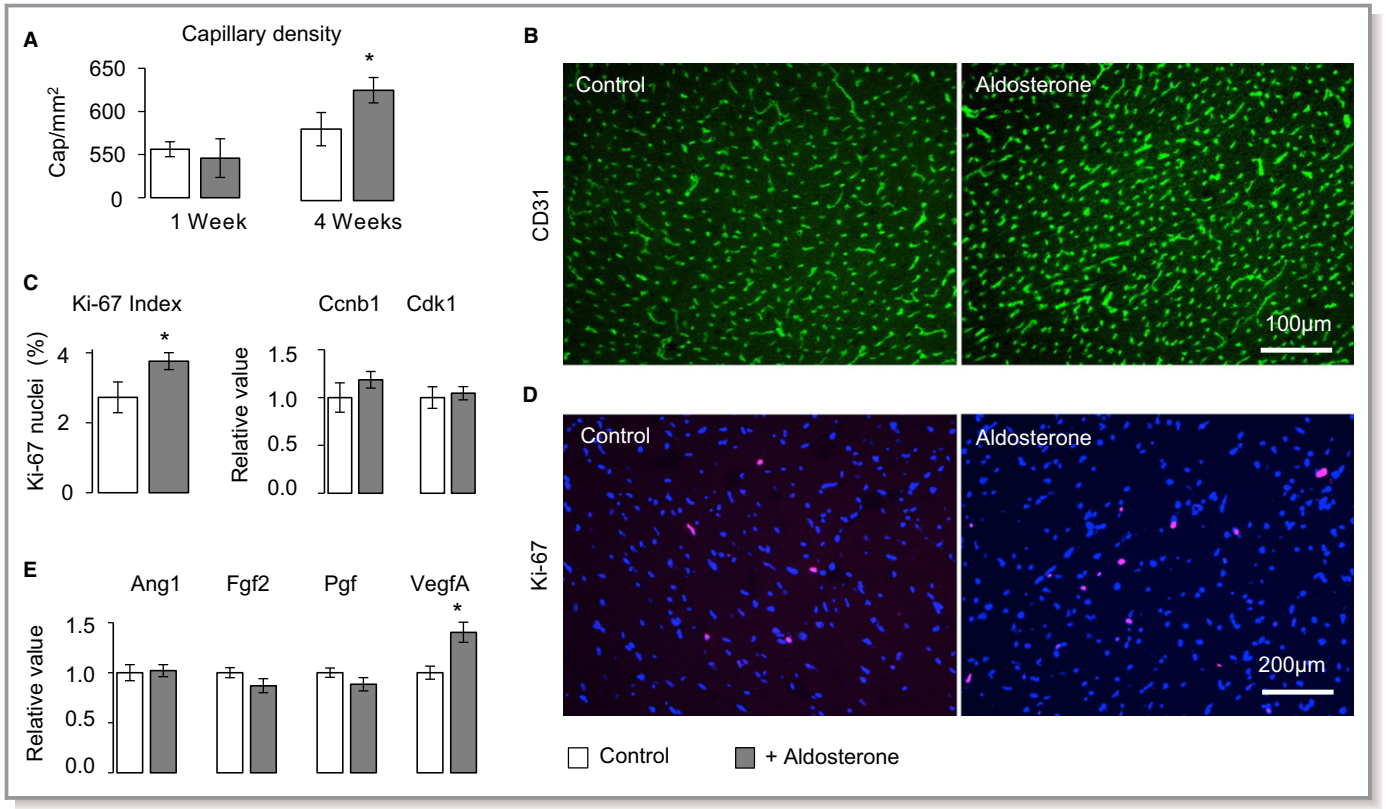

Figure 5. A, Capillary density. Aldosterone administration did not alter the number of capillaries after 1 week (control n=6 and aldosterone n=9) of treatment. Longer treatment (4 weeks; control n=8 and aldosterone n=8) increased capillary density by 7%. Statistical analysis was performed by Mann–Whitney test. Mean±SEM. *P<0.05 vs corresponding controls. B, Immunolabeling of cardiac sections from untreated and aldosterone-treated mice following 4 weeks of treatment. Cardiac sections (4 µm) were labeled with anti-CD31 antibody. C and D, Cardiac cell proliferation. C, Aldosterone induced an increase in cardiac Ki-67 index in mice after 4 weeks of treatment; however, cardiac expression of cyclin B1 (*Ccnb1*) and cyclin dependant kinase 1 (*Cdk1*) genes was not increased (control n=8 and aldosterone n=8). Statistical analysis was performed by Mann–Whitney test. Mean±SEM. *P<0.05 vs controls. D, Ki-67 immunolabeling of cardiac sections (4 µm) of untreated and aldosterone-treated mice (4 weeks). In blue, DAPI-stained nuclei; in red, Ki-67–positive nuclei. E, Change in transcript expression after 4 weeks aldosterone infusion. Among the proangiogenic factors tested at 1 week (*Ang1*, *Fgf2*, *Pgf*, and *VegfA*), only *VegfA* was increased after 4 weeks of aldosterone treatment (control n=8 and aldosterone n=8). Expression of these genes was assessed by quantitative real-time polymerase chain reaction (normalized to 18S and ubiquitin C genes). Statistical analysis was performed by Mann–Whitney test. Mean±SEM. *P<0.05 vs controls. *Ang1* indicates angiopoietin1; *Fgf2*, fibroblast growth factor 2; *Pgf*, placental growth factor; Q-PCR, quantitative real-time polymerase chain reaction; *Vegf-a*, vascular endothelial growth factor A.

collaborators showed that noncardiomyocyte cell proliferation is involved in the cardiac remodeling occurring in hypertrophic cardiomyopathy,[25] and although the authors did not address the question of the cell type that proliferates, they speculated on cardiac ECs undergoing endothelial-to-mesenchymal transformation, a recognized mechanism involved in cardiac fibrosis.[26] EC environment (healthy or pathological) may determine the fate of aldosterone-activated ECs into neocapillaries or fibroblasts. This hypothesis deserves consideration and needs further investigation.

The mechanisms underlying the proliferative effect of aldosterone on ECs have yet to be established. Aldosterone enhances the expression of proangiogenic factors such as VEGFA[19] or placental growth factor, a member of VEGF family.[27] In our study, expression of *VegfA* and *Pgf* mRNA and of other proangiogenic factors (Ang1 and Fgf2)[28] was not altered after 1 week of treatment, whereas EC proliferation was clearly enhanced (although expression of *VegfA* was increased after 4 weeks, likely to consolidate the newly formed capillaries). This suggests that the primary trigger for aldosterone-induced EC proliferation may not be through proangiogenic growth factors. Direct activation of ECs should be considered. Indeed, aldosterone acts as a growth-promoting factor for different cell types (renal mesangial cells[29] but also vascular smooth muscle cells[30] and cardiac fibroblasts[31]) by promoting the activation of protein kinase signaling cascades.[30,31] It is possible that aldosterone could directly induce EC proliferation in vivo. Stimulation of inflammation and oxidative stress, which are known to induce angiogenesis,[32] is another mechanism that may be involved. Experimentally, the proliferation of vessels in a model of oxygen-induced retinopathy has been associated with the proinflam-

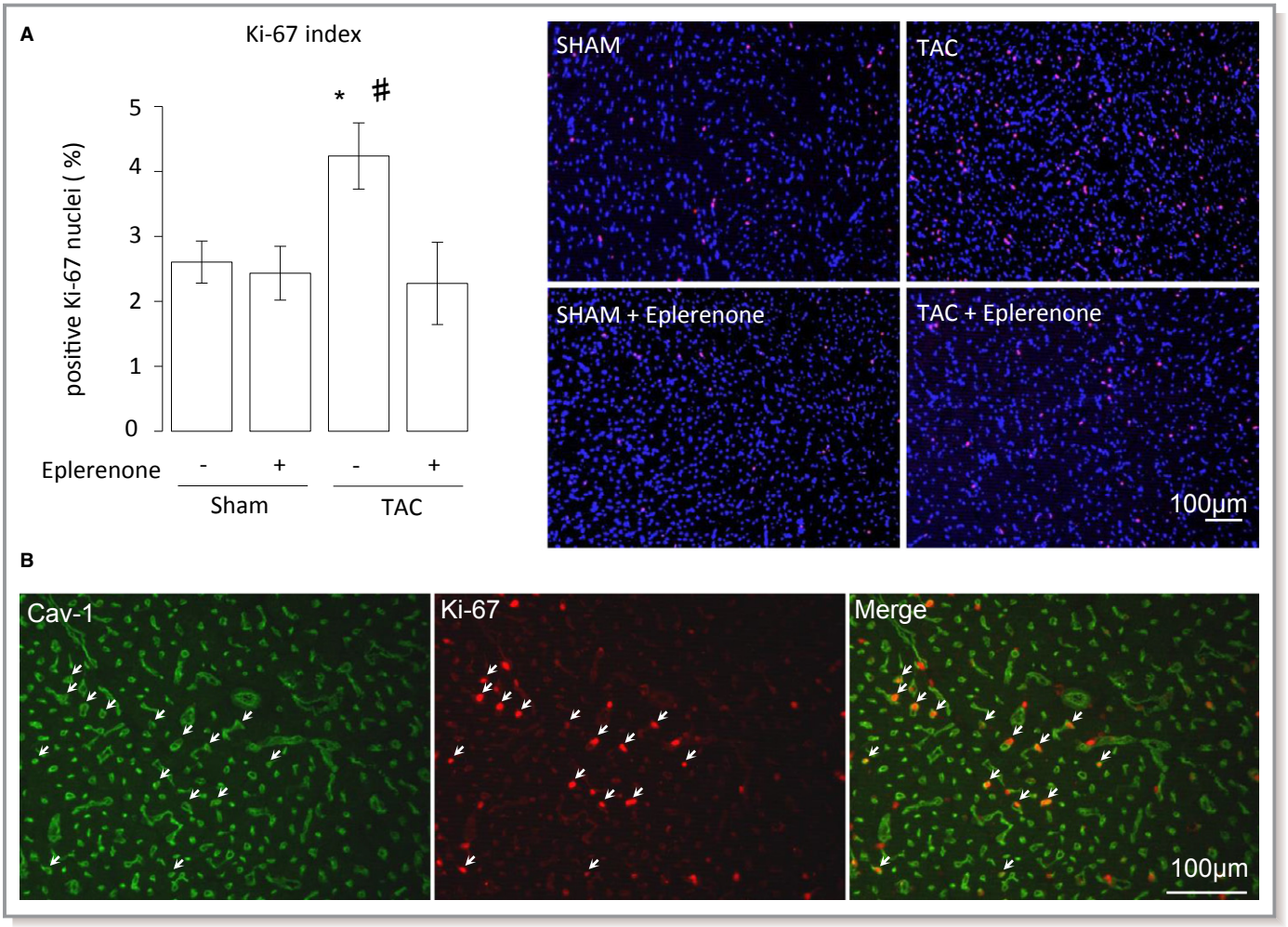

Figure 6. Cell proliferation in a model of heart failure. A, Ki-67 immunolabeling of cardiac sections (in blue, DAPI [4′,6-diamidino-2-phenylindole]-stained nuclei; in red, Ki-67 positive nuclei). TAC induced an increase of Ki-67 index, an effect reversed by eplerenone (sham n=5, sham plus eplerenone n=4, TAC n=5, and TACplus eplerenone n=6). Statistical analysis was performed by Kruskal–Wallis test. The Holm post hoc test was used to adjust for multiple comparisons. Mean±SEM. *$P<0.05$ vs sham, $^{\#}P<0.05$ vs TAC plus eplerenone. B, Double immunolabeling of cardiac sections from rats with TAC. Cardiac sections were labeled with anti-Ki-67 and Cav-1. A very large fraction of Ki-67–positive nuclei colocalized within Cav-1 positive cells, indicating that most of the activated cells were endothelial cells. Cav-1 indicates caveolin 1; TAC, thoracic aortic constriction.

matory properties of aldosterone. In this model, TNF-α, MCP-1, ICAM-1, and VCAM-1 mRNA levels were increased in the retina.[15] In our study, we did not find any effect of aldosterone on the expression of these molecules or pro-oxidative enzymes such as NADPH oxidase (data not shown). It is possible that aldosterone may activate distinct angiogenic pathways according to the vascular microenvironment. We propose that pathological situations may alter the balance between deleterious and beneficial actions of aldosterone, depending on the pathology and the target organ or tissue.

Angiogenesis is a beneficial process in cardiac hypertrophy and ischemic heart diseases.[33] In a transgenic model of cardiac hypertrophy, decrease in cardiac function was accompanied by impaired coronary angiogenesis.[34] Experimentally and clinically, MR antagonists have proven their efficacy in the treatment of heart failure, whether of ischemic origin or not.[35] The beneficial effects of aldosterone blockade are multiple and include antifibrotic and antiarrhythmic properties. Consequently, it is likely that, in these pathological conditions, the deleterious effects of aldosterone overwhelm its positive effects, explaining the beneficial effects of aldosterone antagonists. This may not be the case in all pathological situations. We previously reported that the proangiogenic effects of aldosterone are beneficial in diabetic cardiomyopathy.[20] We demonstrated that a moderate increase of cardiac aldosterone (similar to what achieved in the present study) prevents the capillary rarefaction induced by diabetes, an effect blocked by the MR antagonist eplerenone. Spironolactone, another MR antagonist, has been reported to worsen endothelial function in type 2 diabetic patients.[36] It is possible that in some

pathological situations such as diabetes, such adverse effects of aldosterone antagonists (besides hyperkalemia) need to be taken into account. In contrast, aldosterone-driven angiogenesis may also be deleterious in pathologies such as cancer, in which angiogenesis is essential for tumor growth and metastasis. Little is known about the involvement of MR and aldosterone in tumoral angiogenesis. In humans, aldosterone-producing adenoma vascularization is positively associated with aldosterone levels[37] whereas eplerenone attenuates hepatocellular carcinoma growth and angiogenesis in mice.[38] In contrast, in colorectal cancer, decrease in tumoral MR expression is associated with increased tumoral angiogenesis.[39] Further understanding of the role of aldosterone on cardiovascular homeostasis is required to identify potential adverse effects and new therapeutic potential of aldosterone antagonists to allow more efficient and safer use of these drugs.

This study demonstrates, for the first time, that aldosterone induces cardiac EC cycling in vivo in the heart of normal mice. These findings reveal new perspectives on the role played by aldosterone in cardiac physiology and pathology and highlight potential benefits and concerns with regard to pathologies in which beneficial or deleterious angiogenesis is involved.

Acknowledgments

We thank Prof Iris Z Jaffe (Molecular Cardiology Research Institute, Tufts Medical Center, Boston, MA) for valuable suggestions to the manuscript.

Sources of Funding

This work was supported by grants from INSERM (Institut National pour la Santé et Recherche Médicale), the Agence Nationale pour la Recherche (ANR005-PCOD005 and ANR09-BLAN-0156-01), the European Union (FP7 funded Fibrotarget project SP7#602904) and the CRIT (Centre de Recherche Industrielle et Technique). Messaoudi received grants from the Region île de France (CODDIM) and Societé Française d'Hypertension Arterielle (SFHTA).

Disclosures

None.

References

1. Pitt B, Zannad F, Remme WJ, Cody R, Castaigne A, Perez A, Palensky J, Wittes J. The effect of spironolactone on morbidity and mortality in patients with severe heart failure. Randomized Aldactone Evaluation Study Investigators. *N Engl J Med*. 1999;341:709–717.
2. Pitt B, Remme W, Zannad F, Neaton J, Martinez F, Roniker B, Bittman R, Hurley S, Kleiman J, Gatlin M. Eplerenone, a selective aldosterone blocker, in patients with left ventricular dysfunction after myocardial infarction. *N Engl J Med*. 2003;348:1309–1321.
3. Zannad F, McMurray JJ, Krum H, van Veldhuisen DJ, Swedberg K, Shi H, Vincent J, Pocock SJ, Pitt B. Eplerenone in patients with systolic heart failure and mild symptoms. *N Engl J Med*. 2011;364:11–21.
4. Brilla CG, Pick R, Tan LB, Janicki JS, Weber KT. Remodeling of the rat right and left ventricles in experimental hypertension. *Circ Res*. 1990;67:1355–1364.
5. Sun Y, Zhang J, Lu L, Chen SS, Quinn MT, Weber KT. Aldosterone-induced inflammation in the rat heart: role of oxidative stress. *Am J Pathol*. 2002;161:1773–1781.
6. Johar S, Cave AC, Narayanapanicker A, Grieve DJ, Shah AM. Aldosterone mediates angiotensin II-induced interstitial cardiac fibrosis via a Nox2-containing NADPH oxidase. *FASEB J*. 2006;20:1546–1548.
7. Perrier R, Richard S, Sainte-Marie Y, Rossier BC, Jaisser F, Hummler E, Benitah JP. A direct relationship between plasma aldosterone and cardiac L-type Ca^{2+} current in mice. *J Physiol*. 2005;569:153–162.
8. Gomez AM, Rueda A, Sainte-Marie Y, Pereira L, Zissimopoulos S, Zhu X, Schaub R, Perrier E, Perrier R, Latouche C, Richard S, Picot MC, Jaisser F, Lai FA, Valdivia HH, Benitah JP. Mineralocorticoid modulation of cardiac ryanodine receptor activity is associated with downregulation of FK506-binding proteins. *Circulation*. 2009;119:2179–2187.
9. Milliez P, Girerd X, Plouin PF, Blacher J, Safar ME, Mourad JJ. Evidence for an increased rate of cardiovascular events in patients with primary aldosteronism. *J Am Coll Cardiol*. 2005;45:1243–1248.
10. Messaoudi S, Gravez B, Tarjus A, Pelloux V, Ouvrard-Pascaud A, Delcayre C, Samuel J, Launay JM, Sierra-Ramos C, Alvarez de la Rosa D, Clement K, Farman N, Jaisser F. Aldosterone-specific activation of cardiomyocyte mineralocorticoid receptor in vivo. *Hypertension*. 2013;61:361–367.
11. Latouche C, Sainte-Marie Y, Steenman M, Castro Chaves P, Naray-Fejes-Toth A, Fejes-Toth G, Farman N, Jaisser F. Molecular signature of mineralocorticoid receptor signaling in cardiomyocytes: from cultured cells to mouse heart. *Endocrinology*. 2010;151:4467–4476.
12. Prifti E, Zucker JD, Clement K, Henegar C. FunNet: an integrative tool for exploring transcriptional interactions. *Bioinformatics*. 2008;24:2636–2638.
13. Gerdes J, Lemke H, Baisch H, Wacker HH, Schwab U, Stein H. Cell cycle analysis of a cell proliferation-associated human nuclear antigen defined by the monoclonal antibody Ki-67. *J Immunol*. 1984;133:1710–1715.
14. Hendzel MJ, Wei Y, Mancini MA, Van Hooser A, Ranalli T, Brinkley BR, Bazett-Jones DP, Allis CD. Mitosis-specific phosphorylation of histone H3 initiates primarily within pericentromeric heterochromatin during G2 and spreads in an ordered fashion coincident with mitotic chromosome condensation. *Chromosoma*. 1997;106:348–360.
15. Deliyanti D, Miller AG, Tan G, Binger KJ, Samson AL, Wilkinson-Berka JL. Neovascularization is attenuated with aldosterone synthase inhibition in rats with retinopathy. *Hypertension*. 2012;59:607–613.
16. Thum T, Schmitter K, Fleissner F, Wiebking V, Dietrich B, Widder JD, Jazbutyte V, Hahner S, Ertl G, Bauersachs J. Impairment of endothelial progenitor cell function and vascularization capacity by aldosterone in mice and humans. *Eur Heart J*. 2011;32:1275–1286.
17. Ladage D, Schutzeberg N, Dartsch T, Krausgrill B, Halbach M, Zobel C, Muller-Ehmsen J. Hyperaldosteronism is associated with a decrease in number and altered growth factor expression of endothelial progenitor cells in rats. *Int J Cardiol*. 2011;149:152–156.
18. Wu VC, Lo SC, Chen YL, Huang PH, Tsai CT, Liang CJ, Kuo CC, Kuo YS, Lee BC, Wu EL, Lin YH, Sun YY, Lin SL, Chen JW, Lin SJ, Wu KD. Endothelial progenitor cells in primary aldosteronism: a biomarker of severity for aldosterone vasculopathy and prognosis. *J Clin Endocrinol Metab*. 2011;96:3175–3183.
19. Michel F, Ambroisine ML, Duriez M, Delcayre C, Levy BI, Silvestre JS. Aldosterone enhances ischemia-induced neovascularization through angiotensin II-dependent pathway. *Circulation*. 2004;109:1933–1937.
20. Messaoudi S, Milliez P, Samuel JL, Delcayre C. Cardiac aldosterone overexpression prevents harmful effects of diabetes in the mouse heart by preserving capillary density. *FASEB J*. 2009;23:2176–2185.
21. Wilkinson-Berka JL, Tan G, Jaworski K, Miller AG. Identification of a retinal aldosterone system and the protective effects of mineralocorticoid receptor antagonism on retinal vascular pathology. *Circ Res*. 2009;104:124–133.
22. Brutsaert DL. Cardiac endothelial-myocardial signaling: its role in cardiac growth, contractile performance, and rhythmicity. *Physiol Rev*. 2003;83:59–115.
23. Caprio M, Newfell BG, la Sala A, Baur W, Fabbri A, Rosano G, Mendelsohn ME, Jaffe IZ. Functional mineralocorticoid receptors in human vascular endothelial cells regulate intercellular adhesion molecule-1 expression and promote leukocyte adhesion. *Circ Res*. 2008;102:1359–1367.

24. Kirsch T, Beese M, Wyss K, Klinge U, Haller H, Haubitz M, Fiebeler A. Aldosterone modulates endothelial permeability and endothelial nitric oxide synthase activity by rearrangement of the actin cytoskeleton. *Hypertension*. 2013;61:501–508.
25. Teekakirikul P, Eminaga S, Toka O, Alcalai R, Wang L, Wakimoto H, Nayor M, Konno T, Gorham JM, Wolf CM, Kim JB, Schmitt JP, Molkentin JD, Norris RA, Tager AM, Hoffman SR, Markwald RR, Seidman CE, Seidman JG. Cardiac fibrosis in mice with hypertrophic cardiomyopathy is mediated by non-myocyte proliferation and requires Tgf-beta. *J Clin Invest*. 2010;120:3520–3529.
26. Zeisberg EM, Tarnavski O, Zeisberg M, Dorfman AL, McMullen JR, Gustafsson E, Chandraker A, Yuan X, Pu WT, Roberts AB, Neilson EG, Sayegh MH, Izumo S, Kalluri R. Endothelial-to-mesenchymal transition contributes to cardiac fibrosis. *Nat Med*. 2007;13:952–961.
27. Jaffe IZ, Newfell BG, Aronovitz M, Mohammad NN, McGraw AP, Perreault RE, Carmeliet P, Ehsan A, Mendelsohn ME. Placental growth factor mediates aldosterone-dependent vascular injury in mice. *J Clin Invest*. 2010;120:3891–3900.
28. Papetti M, Herman IM. Mechanisms of normal and tumor-derived angiogenesis. *Am J Physiol Cell Physiol*. 2002;282:C947–C970.
29. Nishiyama A, Yao L, Fan Y, Kyaw M, Kataoka N, Hashimoto K, Nagai Y, Nakamura E, Yoshizumi M, Shokoji T, Kimura S, Kiyomoto H, Tsujioka K, Kohno M, Tamaki T, Kajiya F, Abe Y. Involvement of aldosterone and mineralocorticoid receptors in rat mesangial cell proliferation and deformability. *Hypertension*. 2005;45:710–716.
30. Ishizawa K, Izawa Y, Ito H, Miki C, Miyata K, Fujita Y, Kanematsu Y, Tsuchiya K, Tamaki T, Nishiyama A, Yoshizumi M. Aldosterone stimulates vascular smooth muscle cell proliferation via big mitogen-activated protein kinase 1 activation. *Hypertension*. 2005;46:1046–1052.
31. Stockand JD, Meszaros JG. Aldosterone stimulates proliferation of cardiac fibroblasts by activating Ki-RasA and MAPK1/2 signaling. *Am J Physiol Heart Circ Physiol*. 2003;284:H176–H184.
32. Kim YW, West XZ, Byzova TV. Inflammation and oxidative stress in angiogenesis and vascular disease. *J Mol Med (Berl)*. 2013;91:323–328.
33. Oka T, Akazawa H, Naito AT, Komuro I. Angiogenesis and cardiac hypertrophy: maintenance of cardiac function and causative roles in heart failure. *Circ Res*. 2014;114:565–571.
34. Shiojima I, Sato K, Izumiya Y, Schiekofer S, Ito M, Liao R, Colucci WS, Walsh K. Disruption of coordinated cardiac hypertrophy and angiogenesis contributes to the transition to heart failure. *J Clin Invest*. 2005;115:2108–2118.
35. Messaoudi S, Azibani F, Delcayre C, Jaisser F. Aldosterone, mineralocorticoid receptor, and heart failure. *Mol Cell Endocrinol*. 2012;350:266–272.
36. Davies JI, Band M, Morris A, Struthers AD. Spironolactone impairs endothelial function and heart rate variability in patients with type 2 diabetes. *Diabetologia*. 2004;47:1687–1694.
37. Bernini GP, Moretti A, Bonadio AG, Menicagli M, Viacava P, Naccarato AG, Iacconi P, Miccoli P, Salvetti A. Angiogenesis in human normal and pathologic adrenal cortex. *J Clin Endocrinol Metab*. 2002;87:4961–4965.
38. Kaji K, Yoshiji H, Kitade M, Ikenaka Y, Noguchi R, Shirai Y, Yoshii J, Yanase K, Namisaki T, Yamazaki M, Tsujimoto T, Kawaratani H, Fukui H. Selective aldosterone blocker, eplerenone, attenuates hepatocellular carcinoma growth and angiogenesis in mice. *Hepatol Res*. 2010;40:540–549.
39. Tiberio L, Nascimbeni R, Villanacci V, Casella C, Fra A, Vezzoli V, Furlan L, Meyer G, Parrinello G, Baroni MD, Salerni B, Schiaffonati L. The decrease of mineralcorticoid receptor drives angiogenic pathways in colorectal cancer. *PLoS One*. 2013;8:e59410.